ABCM Symposium Series in Bioengineering, Vol. 1

SEM OBSERVATIONS AND ELECTROCHEMICAL BEHAVIOUR OF A STAINLESS STEEL IMPLANT DEVICE - A CASE STUDY

Renato Altobelli Antunes
Institution and address: Instituto de Pesquisas Energéticas e Nucleares (IPEN/CNEN-SP) Av. Prof. Lineu Prestes 2242 - Cidade Universitária - São Paulo - SP - 05508-900
e-mail: rantunes@ipen.br

Maysa Terada
Institution and address: Instituto de Pesquisas Energéticas e Nucleares (IPEN/CNEN-SP) Av. Prof. Lineu Prestes 2242 - Cidade Universitária - São Paulo - SP - 05508-900
e-mail: maysaterada@uol.com.br

Isolda Costa
Institution and address: Instituto de Pesquisas Energéticas e Nucleares (IPEN/CNEN-SP) Av. Prof. Lineu Prestes 2242 - Cidade Universitária - São Paulo - SP - 05508-900
e-mail: icosta@ipen.br

Abstract. *Austenitic stainless steels are widely used for biomedical devices both temporary or long-term applications. However, it is frequently reported that these steels are prone to localized attack when immersed in biological fluids and that their corrosion products may lead to allergenic or infectious reactions when in contact with human tissues. The investigation of implants surface after removal from the patient may lead to valuable information about possible degradation during the implantation period. The understanding of the degradation mechanisms may lead to the development of implant materials with improved corrosion resistance and biocompatibility. The aim of this work was to assess the surface morphology and the corrosion resistance of a stainless steel plate device for internal fixation of long fractured bones explanted from the patient after 26 months. Scanning electron microscopy (SEM) was used for the surface observations. Corrosion tests were performed in Hanks' physiological solution at 25ºC using specimens cut from the explanted bone plate. The immersion period was up to 7 days. Electrochemical impedance spectroscopy and potentiodynamic polarization were used as investigation techniques. The results indicated that the explant device did not present significant signs of corrosion attack as shown in the SEM micrographs. There were signs of mechanical deformation. The corrosion resistance was similar to that of the same material before implantation.*

Keywords*: corrosion resistance, stainless steel F138, internal fixation plate*

1. Introduction

Austenitic stainless steels are commonly used for biomedical applications but present poorer corrosion resistance when compared to other metallic biomaterials such as cobalt-chrome and titanium alloys (Nielsen 1987, Walzack, Shahgaldi.and Heatley 1998). Several works in the literature report on the localized corrosion of stainless steel implants (Zabel et al., 1988, Sivakumar, Mudali and Rajeswari 1994, Gurappa 2002, Assis et al., 2005). Corrosion products released to the human body may lead to infectious reactions that make the patient undergoes additional suffering ultimately leading to implant failure (Pereira et al., 1995). However, these materials are still used as implants due to low cost and suitable mechanical resistance (Meinert et al., 1998). The aim of this work was to assess the deterioration of a stainless steel implant device used as an internal fixation plate for long fractured bones. The device was explanted from the patient after 26 months of implantation and its surface was observed using scanning electron microscopy (SEM). The corrosion resistance of the explanted implant was evaluated by means of electrochemical impedance spectroscopy (EIS) and potentiodynamic polarization curves.

2. Experimental

The stainless steel fixation plate tested in this work was purchased by the Brazilian Public Health Service (SUS – Sistema Único de Saúde) and the material used in its preparation was identified as ASTM F-138 stainless steel.

Electrochemical Measurements
The experiments were performed on the plate surface itself as explanted from the patient, leaving an exposure area to the electrolyte of approximately 0.39 cm^2, without any surface grinding or polishing. The plate was properly sterilized, degreased with acetone and rinsed in deionized water before the tests. The specimen remained immersed for 24 hours in Hanks' solution, naturally aerated at 25 ºC, prior to the tests.
A three-electrode cell arrangement was used for the electrochemical measurements, with a saturated calomel reference electrode (SCE) as reference electrode and a platinum wire as the auxiliary electrode. The electrolyte used to simulate the physiological medium was Hanks' solution, naturally aerated (pH=6.8) and its composition is presented in Tab. 1. The period of immersion was up to 7 days at 25ºC.

Table 1. Chemical composition of Hank's solution.

Component	Concentration (Mol/L)
NaCl	0.1369
KCl	0.0054
$MgSO_4.7H_2O$	0.0008
$CaCl_2.2H_2O$	0.0013
$Na_2HPO_4.2H_2O$	0.0003
KH_2PO_4	0.0004
$C_6H_{12}O_6H_2O$	0.0050
Red phenol 1%	0.0071
pH	6.8

EIS measurements were carried out with a frequency response analyser (Solartron SI-1255) coupled to a potentiostat (EG&G PARC 273A). All EIS measurements were performed in potentiostatic mode at the corrosion potential (E_{corr}). The perturbation signal amplitude was 10 mV, and the frequency range of investigation varied from 10^{-2} Hz to 10^{5} Hz with an acquisition rate of 6 points per decade.

Potentiodynamic polarization curves were obtained after 7 days of immersion in Hanks' solution at 25 ºC, using a scanning rate of 1 mV.s^{-1}. A potentiostat/galvanostat EG&G 273A was used for the measurements, starting at -800 mV_{SCE} and finishing at 3000 mV_{SCE}.

SEM observations

SEM-analyses were performed with a Philips XL30 microscope on specimens cut from the explanted stainless steel fixation plate.

3. Results and Discussion

Figure 1 shows a partial radiograph of the implanted plate attached to the femur of the patient.

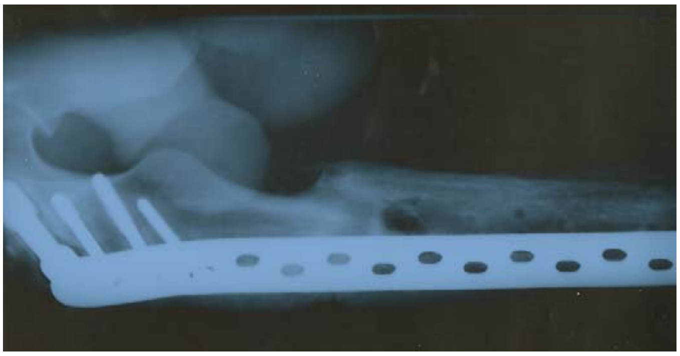

Figure 1. Radiograph of the implanted stainless steel F138 plate before removal from the patient.

The plate removed from a patient after 26 months is shown in Fig. 2a. There are visible signs of mechanical deformation on the right side of the plate that may have been introduced during the implantation or the removal from the patient. These signs are shown in detail in Fig. 2b. On the other hand there were no visible signs of corrosion on the plate surface.

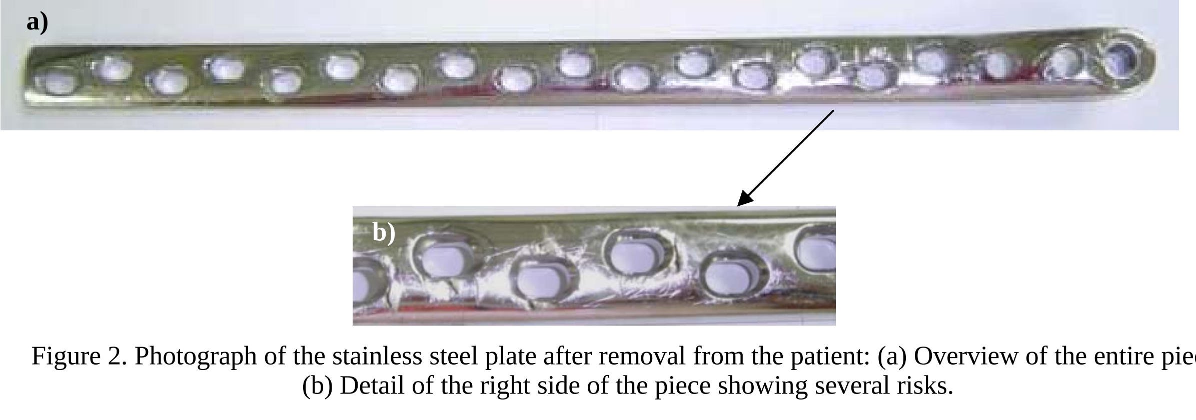

Figure 2. Photograph of the stainless steel plate after removal from the patient: (a) Overview of the entire piece; (b) Detail of the right side of the piece showing several risks.

SEM micrographs of the plate are shown in Fig. 3. The micrograph on Fig. 3a was taken from a region between the plate holes with few signs of mechanical damage. Even tough, some risks and pinholes are distinguishable on the plate surface. Fig. 3b shows the same region with higher magnification.

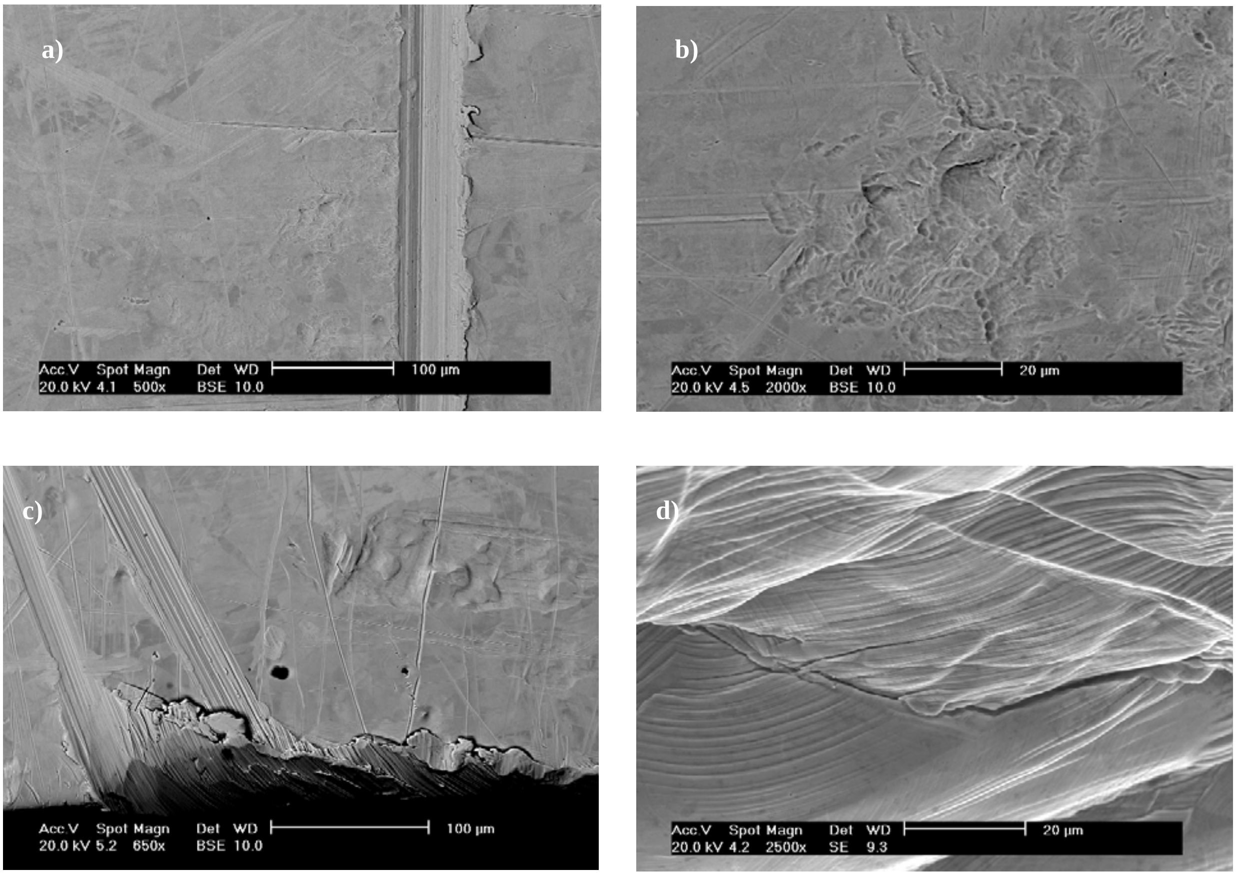

Figure 3. SEM micrographs of the explanted plate: (a) region between plate holes with few signs of deformation; (b) same region of Fig 3a with higher magnification; (c) deformed region near the plate hole; (d) inside the crack of Fig 3c.

A more severely damaged region near the board of a plate hole is presented in Fig. 3c. Deep cracks and higher pinholes are seen on plate surface. Fig. 3d shows a region inside one of the small cracks on Fig. 3c. It is not possible to know for sure if the deformation was introduced during the implantation or the removal of the plate. As the plate was removed after bone healing and not due to implant failure it is likely that the severe deformation signs observed in Fig 2 have been introduced during the removal operation rather than the implantation one. This last hypothesis has been acknowledged to discuss the corrosion behaviour of the device.

Before starting to discuss the electrochemical results it is noteworthy to mention that the measurements have been taken directly on the plate surface in the less deformed regions between the plate holes, such as that shown in Fig. 3a. This region was chosen to avoid the more severely damaged sites that were considered to come out from the removal operation of the implant device. The objective was to investigate the corrosion behaviour of the plate as it was placed inside the patient’s body.

EIS diagrams of the explanted plate device up to six days of immersion in Hanks' solution at 25 ºC are shown in Fig. 4a and 4b as Bode and Nyquist plots, respectively. The electrochemical behaviour was highly capacitive through the whole period of immersion. After the first day of immersion, Bode plot (Figure 4a) presents one time constant characterized by a plateau in the middle frequency region with a phase angle value around -80º. This time constant may be ascribed to the impedance response of the defects on the surface oxide layer of the stainless steel plate. The phase diagrams did not change up to 6 days of immersion revealing a highly stable oxide layer in the conditions tested. Nyquist plots (Fig. 4b) present a capacitive loop with high impedance values that slightly decreased with increasing immersion times.

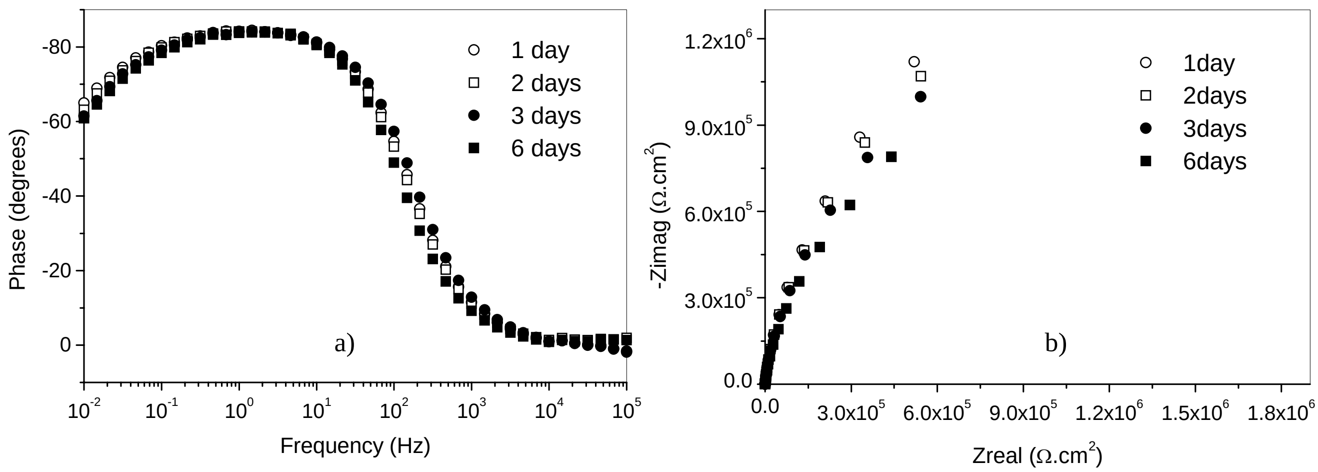

Figure 4. EIS diagrams of the stainless steel plate after 1, 2, 3 and 6 days of immersion in Hanks solution at 25ºC: (a) Bode plots (phase angle) and (b) Nyquist plots.

The potentiodynamic polarization curve of the explanted plate device obtained after 7 days of immersion in Hanks' solution at 25ºC is shown in Fig. 5.

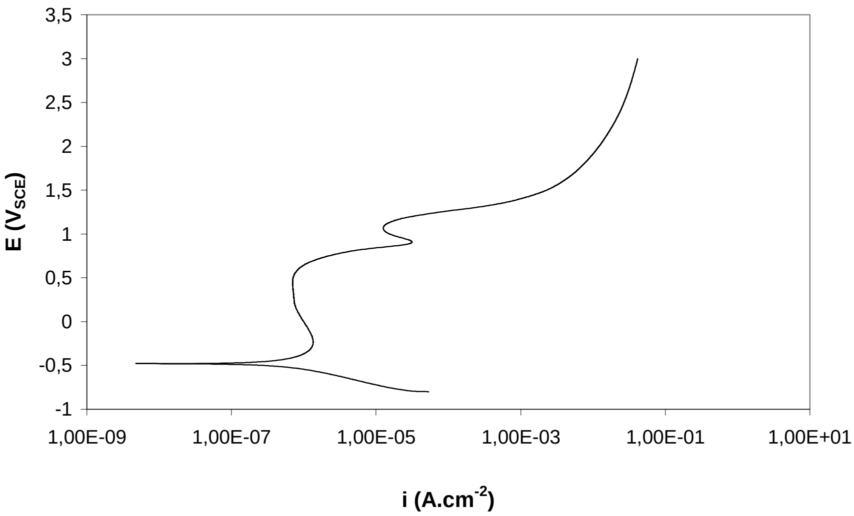

Figure 5. Potentiodynamic polarization curve of the explanted plate device after 7 days of immersion in Hanks' solution at 25ºC.

The result of Fig. 5 shows that the stainless steel plate is prone to pitting corrosion in the Hanks' solution with a breakdown potential around +0.57V due to the onset of pitting corrosion. This assertion was expected and is consistent with other literature reports (Assis et al., 2005, Paschoal et al. 2003). At +0.9V there is a small decrease in the current density followed by a sharp increase at +1.15 V that is likely due to the oxygen evolution reaction. The corrosion potential was -0.48 V. The corrosion current density determined by the extrapolation of the linear cathodic portion of the polarization curve to the corrosion potential (E_{corr}) was 1.13 $\mu A.cm^{-2}$. This small value is consistent with the highly capacitive behaviour observed in the EIS diagrams (Fig. 4) and accounts for a high corrosion resistance of the implant.

4. Conclusions

The explanted stainless steel plate did not present visible signs of corrosion but was highly damaged especially in the areas where the fixation screws had been attached. The device presented high corrosion resistance as determined from the electrochemical measurements but it is prone to localized attack. Furthermore, it is important to keep in mind that the measurements have been made directly on the plate surface in the less deformed regions between the plate holes. It was assumed that the mechanical deformation observed on the plate was mostly introduced during the removal operation and did not act as preferential corrosion sites during the implantation period. However, it is very likely that some risks and cracks had been produced during the implantation of the medical device. In addition, crevices between the plate and the screws may lead to localized corrosion of the implant. The accuracy of the surgeon is of prime importance to avoid excessive mechanical deformation. Another essential feature is the intrinsic corrosion resistance of the implant material.

5. Acknowledgements

The authors are thankful to CNPq and CAPES for the financial support. Dr. Clarice T. Kuniyoshi (Escola Politécnica da USP – Engenharia de Materiais e Metalúrgica – Laboratório de Microscopia Eletrônica) is kindly acknowledged for the SEM micrographs.

6. References

Assis, S. L., Rogero, S. O., Antunes, R. A., Padilha, A. F., Costa, I., 2005, A comparative study of the in vitro corrosion behaviour ad cytotoxicity of a superferritic stainless steel, a Ti-13Nb-13Zr alloy and an austenitic stainless steel in Hank's solution, *Journal of Biomedical Materials Research*, Vol. 73B, pp. 109-116.
Gurappa, I., 2002, Characterization of different materials for corrosion resistance under simulated body fluid conditions, *Materials Characterization*, Vol. 49, pp. 73-79.
Meinert, K., Uerpmann, C., Matschullatt, J., Wolf, G. K., 1998, Corrosion and leaching of silver doped ceramic IBAD coatings on SS 316L under simulated physiological conditions, *Surface and Coatings Technology*, Vol. 103-104, pp. 58.
Nielsen, K., 1987, Corrosion of metallic implants, *British Corrosion Journal*, Vol. 22, pp. 272-278.
Paschoal, A. L., Vanâncio, E. C., Canale, L. C. F., Silva, O. L., Vilca, H-. D., Motheo, A. J., 2003, Metallic biomaterials TiN-coated: corrosion analysis and biocompatibility, *Artificial Organs*, Vol. 27, pp. 461-464.
Pereira, M. L., Abreu, A. M., Sousa, J. P., Carvalho, G. S., 1995, Chromium accumulation and ultrastructural changes in the mouse liver caused by stainless steel corrosion products, *Journal of Materials Science: Materials in Medicine*, Vol. 6, 523-527.
Sivakumar, M., Mudali, U. K., Rajeswari, S., 1994, Investigation of failures in stainless steel orthopaedic implant device, *Steel Research*, Vol. 65, pp. 76-79.
Walzack, J., Shahgaldi, F., Heatley, F., 1998, In vivo corrosion of 316L stainless-steel hip implants: morphology and elemental compositions of corrosion products, *Biomaterials*, Vol. 19, pp. 229-237.
Zabel, D. D., Brown, S. A., Merritt, K., Payer, J. H., 1988, AES analysis of stainless steel corroded in saline, in serum and *in vivo*, *Journal of Biomedical Materials Research*, 1988, Vol. 22, pp. 31-44.

7. Responsibility notice

The authors are the only responsible for the printed material included in this paper.